

## PAPER

# Fabrication of TiO<sub>2</sub> Nanoparticle Coating on Stainless Steel 316L and Its Assessment for Orthopaedic Applications

Manjit Singh Jadon()  
Sandeep Kumar

Department of Bio and  
Nano Technology, Guru  
Jambheshwar University of  
Science and Technology,  
Hisar, Haryana, India

[msjadon1910@gjust.org](mailto:msjadon1910@gjust.org)

## ABSTRACT

The study aims to investigate the efficacy of titanium dioxide (TiO<sub>2</sub>) nanoparticle coating on stainless steel 316L (SS 316L) orthopaedic implants to enhance their biocompatibility, osseointegration, and durability. The TiO<sub>2</sub> nanoparticles were synthesized via the hydrothermal method and extensively characterized for composition, crystallinity, and morphology using techniques such as X-ray diffraction (XRD), Fourier transform infrared spectroscopy (FTIR), and scanning electron microscopy (SEM) with energy dispersive X-ray analysis (EDX), corroborated by elemental mapping. SEM and XRD analyses revealed the synthesized nanoparticles have a spherical shape and an average size of approximately 23 nanometres. The synthesized TiO<sub>2</sub> nanoparticles were uniformly coated on SS 316L substrates using the spin coating technique, as confirmed by SEM images. Cell viability of the synthesized TiO<sub>2</sub> nanoparticles, as well as uncoated and TiO<sub>2</sub> nanoparticle-coated SS 316L substrates, was evaluated using the MTT (3-(4, 5-dimethylthiazol-2-yl)-2, 5-diphenyltetrazolium bromide) assay against the NIH-3T3 mouse embryonic fibroblast cell line. The results demonstrated that the TiO<sub>2</sub> nanoparticle-coated SS 316L substrate showed a significant increase of 22.87% in cell viability as compared to the uncoated SS 316L substrate. A ball-on-disc tribometer was employed to assess wear and friction resistance at various speeds, viz., 150 rpm, 300 rpm, and 450 rpm, under 30N load conditions for five minutes. The results collectively indicate a substantial improvement in the performance of TiO<sub>2</sub> nanoparticle-coated SS 316L substrates for orthopaedic applications.

## KEYWORDS

nanoparticles, titanium dioxide, stainless steel, orthopaedic implants, biocompatibility, durability, cytotoxicity

## 1 INTRODUCTION

Orthopaedic implants represent a cornerstone of modern medical technology, providing invaluable support in restoring mobility and alleviating pain for

Jadon, M.S., Kumar, S. (2024). Fabrication of TiO<sub>2</sub> Nanoparticle Coating on Stainless Steel 316L and Its Assessment for Orthopaedic Applications. *International Journal of Online and Biomedical Engineering (iJOE)*, 20(10), pp. 47–63. <https://doi.org/10.3991/ijoe.v20i10.49177>

Article submitted 2024-03-18. Revision uploaded 2024-04-26. Final acceptance 2024-04-26.

© 2024 by the authors of this article. Published under CC-BY.

individuals grappling with musculoskeletal disorders, including osteoarthritis, fractures, and joint degeneration. These implants serve as essential tools for enhancing both function and quality of life for patients worldwide [1]. In the realm of orthopaedic implant metals, stainless steel has long been used for its exceptional mechanical strength, corrosion resistance, durability, and cost-effectiveness. However, despite their widespread use, stainless steel implants are not without their challenges [2]. Some of the major drawbacks include poor wear resistance, a low fatigue strength, low osseointegration rate, high stress shielding, and a higher elastic modulus. Biocompatibility issues often arise, posing significant hurdles that can lead to complications such as inflammation, implant loosening, and ultimately implant failure [3]. Also, the long-term implications of stainless steel (SS 316L) are that it is susceptible to chemical and biological reactions, resulting in the release of metal ions that can accumulate around the implant and induce inflammation. Addressing these challenges is paramount to ensuring the long-term success and efficacy of orthopaedic interventions. Recognizing the need for innovative solutions, researchers have turned to surface modifications as a promising avenue for improving the performance of stainless-steel implants [4]. Various surface modification techniques, viz., surface coating, plasma spraying, physical and chemical vapour deposition, ion implantation, surface roughening, functionalization, and biomimetic coatings, have been extensively used to enhance their performance and durability. Among these modifications, nanoparticle coatings have garnered considerable attention for their unique ability to tailor surface properties and interactions with biological tissues. In the last few decades, nanoparticles have attracted attention for their potential as coating materials for biomedical applications. Among all the nanomaterials, metal, metal oxide, composite and ceramic nanomaterials have shown great promise for their antimicrobial efficiency, biocompatibility, mechanical strength, wear resistance and corrosion resistance. The selection of nanoparticles to be coated depends on the desired functionality. Numerous investigations have demonstrated the exceptional antimicrobial properties of silver nanoparticles (Ag NPs), which efficiently eradicate bacteria, thus mitigating infection and inflammation. Copper oxide nanoparticles (CuO NPs) have been examined for their potential in anticancer therapy and treatment. Zinc oxide nanoparticles (ZnO NPs) have exhibited notable antibacterial efficacy and biocompatibility. Combinations of titanium dioxide (TiO<sub>2</sub>) and zinc oxide (ZnO) in nanocomposites have demonstrated antibacterial effects against *Escherichia coli*. Magnesium oxide (MgO) nanoparticles have exhibited enhanced mechanical strength and biocompatibility. Coatings comprising silver-magnesium oxide (Ag-MgO) nanocomposites on stainless steel 316 substrates have exhibited superior antibacterial efficacy, biocompatibility, corrosion resistance, and reduced rates of wear and frictional resistance. In particular, titanium dioxide (TiO<sub>2</sub>) nanoparticles have emerged as a frontrunner in this field, offering a suite of desirable characteristics that make them well-suited for coating orthopaedic implants [5]. TiO<sub>2</sub> nanoparticles possess good tensile strength, high fatigue strength, a low wear rate, and reduced stress shielding. TiO<sub>2</sub> nanoparticles have excellent biocompatibility, rendering them compatible with biological systems and minimizing adverse reactions within the body. Additionally, these nanoparticles exhibit antimicrobial properties, which are particularly crucial in the context of orthopaedic surgery, where the risk of infection is a significant concern [6]. Moreover, TiO<sub>2</sub> nanoparticles demonstrate osseointegration, facilitating the process of osseointegration of an implant [7]. By incorporating TiO<sub>2</sub> nanoparticles, orthopaedic implants made from SS 316L can offer a combination of biocompatibility,

antibacterial properties, corrosion resistance, and bioactivity, thereby improving patient outcomes and expanding the range of applications in orthopaedic surgery [8]. Through precise modulation of surface characteristics, TiO<sub>2</sub> nanoparticle coatings have the potential to foster improved tissue integration, reduce the risk of complications, and ultimately extend the lifespan of orthopaedic implants [9].

Though there are few studies on the antibacterial efficiency of TiO<sub>2</sub> nanoparticles. Our work presents a new perspective within the field of nanoparticle coating on implant surfaces as we studied the efficiency of TiO<sub>2</sub> nanoparticle coating on SS 316L substrate for their biocompatibility, wear resistance and, durability offering a novel approach that differentiates it from existing research in the field. In the present study, we synthesised TiO<sub>2</sub> nanoparticles using the hydrothermal method and characterised them using various characterization techniques. Further, the synthesised TiO<sub>2</sub> nanoparticles were coated on the surface of the SS 316L substrate using the spin coating technique. Our study focuses on characterizing and evaluating the properties of TiO<sub>2</sub> nanoparticles, including biocompatibility, mechanical integrity, wear rate and frictional resistance. We aimed to comprehensively study these aspects to assess the suitability of TiO<sub>2</sub> nanoparticles for various applications, particularly in enhancing the performance of orthopaedic implants. The MTT “3-(4, 5-dimethylthiazol-2-yl)-2, 5-diphenyltetrazolium bromide” assay was used to evaluate the cell viability against the NIH-3T3 mouse embryonic fibroblast cell line to ensure the safety of the TiO<sub>2</sub> nanoparticle coating for clinical use. The ball-on-disc method were utilized to determine the wear rate and frictional resistance of TiO<sub>2</sub> nanoparticle coating on SS 316L substrate at various speeds (150 rpm, 300 rpm, and 450 rpm) under 30N load conditions.

## 2 MATERIALS AND METHODS

### 2.1 Materials

The TiO<sub>2</sub> powder and KOH solvent were purchased from Sigma Aldrich. These chemicals were utilized as received without additional purification.

### 2.2 Preparation of TiO<sub>2</sub> nanoparticles

Prepare a titanium precursor solution by dissolving titania powder in 100 ml of distilled water. Next, dissolve potassium hydroxide (KOH) in another 100 ml of distilled water to form a reducing agent solution. Combine both solutions dropwise while stirring continuously at 500 rpm until complete dissolution is achieved. The reaction mixture was maintained at 50 °C under continuous stirring at 1100 rpm for 24 hours to facilitate the growth of TiO<sub>2</sub> nanoparticles. White precipitates were obtained with the passage of time. The beaker was allowed to stand overnight. Subsequently, remove the supernatant, filter the nanoparticles, and wash them thoroughly using a combination of ethanol and distilled water. Repeat this washing process to ensure the purity of the nanoparticles. Finally, dry the purified TiO<sub>2</sub> nanoparticle suspension at 75 °C to obtain a dry powder form. This powder can then be subjected to calcination at 600 °C for three hours to obtain the desired crystalline TiO<sub>2</sub> nanoparticles [10].

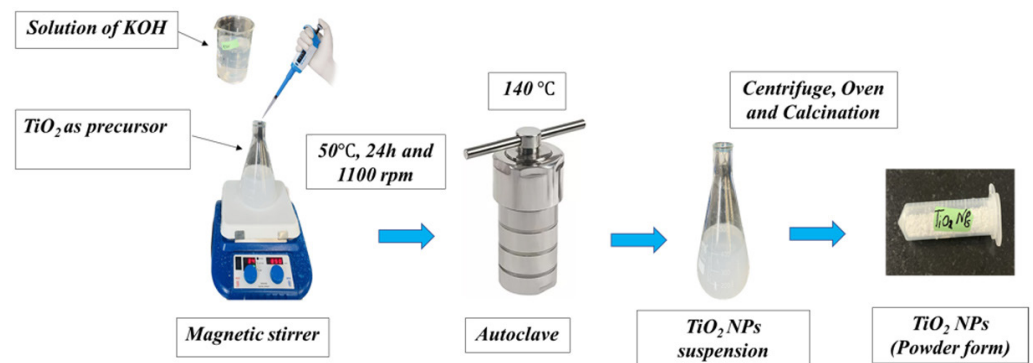


Fig. 1. Synthesis of TiO<sub>2</sub> nanoparticles

### 2.3 Fabrication of SS 316L samples

Stainless steel 316L samples were purchased from Jindal Stainless Hisar Ltd. and used as the substrate for coating. The SS 316L substrate was cut into square sheets measuring  $20 \times 20 \times 1 \text{ mm}^3$ . To eliminate surface imperfections, the substrate sheets were polished using an aluminium slurry, followed by acetone cleaning to remove any remaining surface contaminants, and then rinsed with deionized water to eliminate residual impurities. The samples were then air-dried at 70 °C for 18 hours.

### 2.4 Physiological and morphological characterization techniques

The characterization of synthesised TiO<sub>2</sub> nanoparticles and their coating on stainless steel 316L substrates involves a comprehensive assessment of their physico-chemical properties. This includes examining surface morphology and chemical composition using scanning electron microscopy (SEM FESEM: JEOL, JSM 7610FPlus, Japan). Additionally, X-ray diffraction (XRD: Rigaku Ultima IV system, USA) was utilized to determine the crystalline structure of the coated nanoparticles. Composition and functional group information were acquired using a FTIR (Perkin Elmer, USA), which provides information about the composition and functional group present. The wear rate and friction coefficient were analyzed using a ball-on-disc universal tribometer (DUCOM TR-20 LE).

### 2.5 Fabrication of TiO<sub>2</sub> nanoparticles using spin coating

The spin coating technique was employed to achieve a uniform TiO<sub>2</sub> nanoparticle coating on the SS 316L substrate. Initially, a suspension of TiO<sub>2</sub> nanoparticles was prepared by dispersing 10 milligrams of nanoparticles in 100 ml of distilled water, followed by 24 hours of magnetic stirring for thorough dispersion. Subsequently, the suspension underwent one hour of sonication at room temperature to prevent nanoparticle clustering. Prior to coating, the surface of the SS 316L substrate underwent a chemical etching using a solution of nitric acid and hydrogen peroxide (70:30) to enhance adhesion and promote uniform coating deposition. After etching, the substrate was rinsed with distilled water to remove any residual etchant and then dried thoroughly. The spin coating process comprised three key steps: suspension deposition, spin coating, and drying. Firstly, a flat SS 316L substrate was mounted

onto a spindle, and a liquid nanoparticle solution was dispensed onto its centre using a syringe. The SS 316L substrate was then spun centrifugally at 400 rpm, facilitating uniform spreading of the liquid across the surface. Excess material was expelled from the rotating substrate's edge, ensuring an even coating. Finally, the substrate was left to air dry at 150 °C for two hours to remove solvent residue from its surface [11], [12].

## 2.6 Cell viability

An MTT assay was utilized to evaluate the in vitro cytotoxicity of TiO<sub>2</sub> nanoparticles and both uncoated and coated SS 316L substrates using NIH-3T3 mouse embryonic fibroblast cells. The cells were cultured in DMEM supplemented with 10% FBS and 100 U/ml antibiotic solution, maintained at 37 °C with 5% CO<sub>2</sub>. Cells (1 × 10<sup>6</sup> cells per well) were seeded into P24 microliter plates and exposed to varying concentrations of TiO<sub>2</sub> nanoparticles (100–200 µg/ml) for 48 hours. After incubation, MTT solution (0.5 mg/ml) was added to each well, and cells were further incubated for approximately four hours. The resulting formazan crystals were dissolved in DMSO, and absorbance was measured at 570 nm using a microplate reader. Positive control (untreated cells) and negative control (wells without cells) were included. The same procedure was applied to assess cell viability on uncoated and TiO<sub>2</sub> nanoparticle-coated SS 316L substrates. Relative cell viability was calculated using the provided formulas [13], [14], [15]. All the experiments were performed in triplets.

$$\text{Cell viability (\%)} = (\text{OD Sample} / \text{OD Control}) \times 100\% \quad (1)$$

## 2.7 Wear rate and coefficient of friction

The wear as well as friction parameters of both untreated and TiO<sub>2</sub> nanoparticle coated SS 316L samples were examined using a ball-on-disc tribometer setup. The uncoated and coated SS 316L substrates were joined to various cylindrical SS 316L pieces using metal-to-metal adhesive. The experiments were conducted according to ASTM G99 standards, with rotation speeds of 150 rpm, 300 rpm, and 450 rpm and a constant normal load of 30 N applied for five minutes at room temperature. Before each experiment, thorough cleaning of the ball-on-disc surfaces was performed using ethanol to ensure the removal of any debris or contaminants. The controller was calibrated by setting the values of the LVDT and load cell to zero. During the experiments, both the wear rate and frictional force on the pin were continuously monitored and measured using a linear variable differential transformer and a load cell sensor, respectively [16]. All the experiments were performed in triplets.

# 3 RESULT AND DISCUSSION

## 3.1 XRD (X-Ray Diffraction) analysis

The synthesized TiO<sub>2</sub> nanoparticles underwent X-ray diffraction spectroscopy analysis. XRD is an essential method for studying crystalline structures as it reveals details about the arrangement of atoms within crystals, lattice parameters, and the

size of crystalline domains. Figure 2 illustrates the XRD analysis, revealing diffraction peaks at specific angles: 25.26°, 27.45°, 36.25°, 37.77°, 39.02°, 41.37°, 44.03°, 47.94°, 54.05°, 56.56°, 62.66°, 64.06°, 69.07°, and 69.85°. These peaks correspond to crystallographic planes 101, 110, 103, 004, 200, 111, 210, 200, 105, 220, 002, 310, 310, and 112, respectively, indicating a tetragonal rutile TiO<sub>2</sub> polymorph crystal structure in accordance with DB Card Number 9001681. Scherrer's formula was utilized to determine the average crystalline size of the nanoparticles.

$$D = \beta \cos(\theta) / K\lambda \quad (2)$$

Where, D is the average crystallite size, K is the Scherrer constant (typically around 0.9),  $\lambda$  is the wavelength of the X-ray radiation (1.5406 Å),  $\beta$  is the full width at half maximum (FWHM) of the diffraction peak (in radians), and  $\theta$  is the Bragg angle. The average crystalline size of the synthesized TiO<sub>2</sub> nanoparticles was determined to be 28 nm [13], [14].

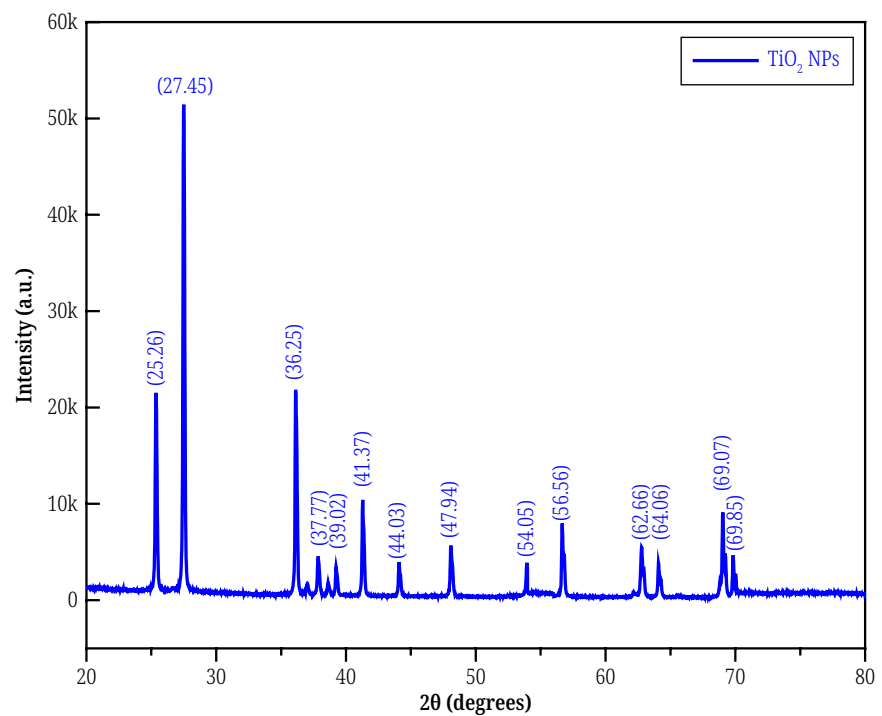


Fig. 2. XRD spectra of TiO<sub>2</sub> nanoparticles

### 3.2 Fourier Transform Infrared Spectroscopy

The FTIR spectrum of the synthesized TiO<sub>2</sub> revealed a transmittance pattern spanning from 4000 cm<sup>-1</sup> to 500 cm<sup>-1</sup>. Through FTIR spectroscopic analysis, the TiO<sub>2</sub> nanoparticles was examined for potential organic functional groups present in the sample. The observed peaks as depicted in Figure 3 were located at specific frequencies: 3423.05 cm<sup>-1</sup>, 1634.74 cm<sup>-1</sup>, 1396.94 cm<sup>-1</sup>, 1085.72 cm<sup>-1</sup>, 811.21 cm<sup>-1</sup>, and 622.09 cm<sup>-1</sup>, corresponding to OH group, C–H stretching and bending, C = O stretching, C–O vibration, C–N stretching group, respectively. Additionally, the absorption peak within the range of 600 cm<sup>-1</sup> corresponds to the Ti–O stretching modes [13], [14].



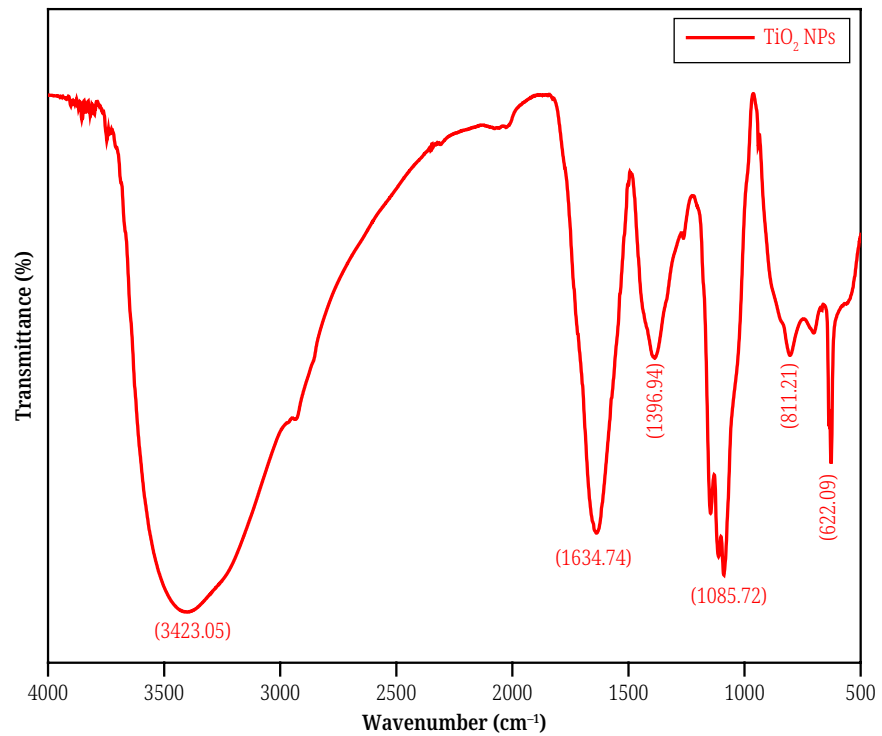


Fig. 3. FTIR spectra of TiO<sub>2</sub> nanoparticles

### 3.3 Scanning electron microscopy analysis

Figure 4 shows the SEM images of the surface morphology of synthesized TiO<sub>2</sub> nanoparticles on coated and uncoated substrate. In SEM micrographs, as depicted in Figure 4a, the morphology of TiO<sub>2</sub> nanoparticles (NPs) reveals the presence of agglomerated, spherical-shaped particles, uniformly distributed. Figure 4b shows a histogram of the size distribution of TiO<sub>2</sub> nanoparticles, which confirmed the mean size of the nanoparticles to be 23 nm. Figure 4c shows the SEM images of the uncoated SS 316L substrate. Figure 4d depicts micrographs of the surface of the TiO<sub>2</sub> nanoparticle coating on the SS 316L substrate, which clearly shows the uniform and dense TiO<sub>2</sub> nanoparticle coating over the SS 316L substrate [11], [13].

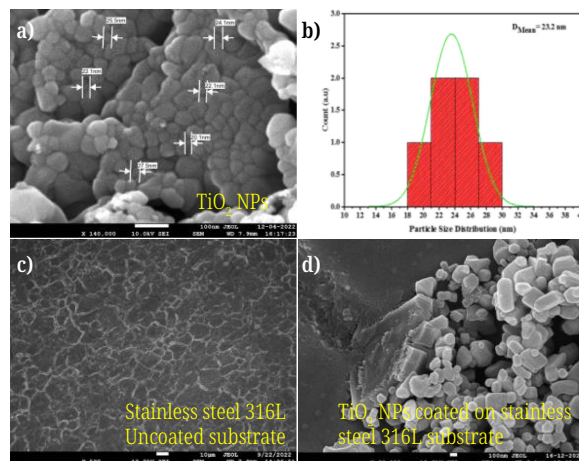
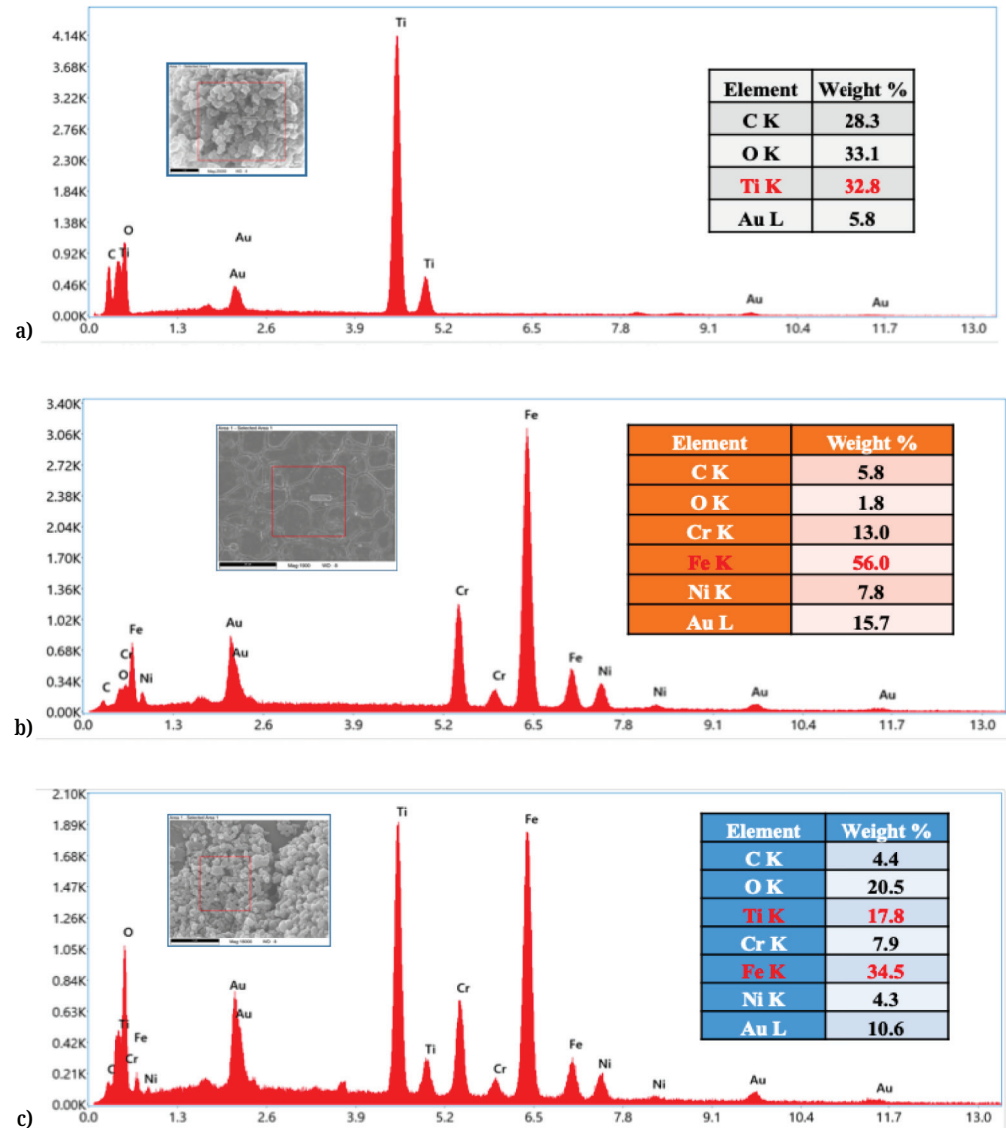


Fig. 4. SEM images of TiO<sub>2</sub> nanoparticles (a), histogram of size distribution of TiO<sub>2</sub> nanoparticles (b), stainless steel 316L uncoated substrate (c), and TiO<sub>2</sub> nanoparticles coated stainless steel 316L substrate (d)

### 3.4 Energy disperse X-ray analysis

Energy-dispersive X-ray spectroscopy (EDX) is a powerful analytical technique used to determine the elemental composition of materials. EDX results confirm the presence and quantify the amounts of titanium, carbon, oxygen, chromium, nickel, iron and gold, oxygen, and iron elements within the TiO<sub>2</sub> nanoparticle coating on the SS 316L substrate. This information is crucial for assessing the quality and composition of the coated material.



**Fig. 5.** Energy disperse X-Ray of TiO<sub>2</sub> nanoparticles (a), stainless steel 316L uncoated substrate (b), and TiO<sub>2</sub> nanoparticles coated stainless steel 316L substrate (c)

The EDX spectrum shown in Figure 5 confirms the presence of TiO<sub>2</sub> nanoparticles (a), uncoated SS 316L substrate (b), and TiO<sub>2</sub> nanoparticles coated SS 316L substrate. TiO<sub>2</sub> nanoparticles reveal the presence of titanium (32.8%), carbon (28.3%), oxygen (33.1%), and gold (5.8%) elements. The uncoated SS 316L substrate shows the presence of iron (56.0%), carbon (5.8%), oxygen (1.8%), chromium (13.0%),



nickel (7.8%) and gold (15.7%). TiO<sub>2</sub> nanoparticles coated with SS 316L substrate are presence of iron (34.5%), carbon (4.4%), oxygen (20.5%), chromium (7.9%), nickel (4.3%), titanium (17.8%), and gold (10.6%) elements. The spectrum provides clear weight percentage data for all elements, confirming the successful coating of TiO<sub>2</sub> nanoparticles onto the substrate [16].

### 3.5 Element mapping

The element mapping results refer to the spatial distribution of different chemical elements within a sample. This technique is often utilized in conjunction with SEM to visualize the distribution of elements across the surface of a material. The resulting data generates a visual representation of the distribution of elements, typically displayed as a color-coded map overlaid onto an image of the sample. Each colour represents a different element, and the intensity of the colour corresponds to the concentration of that element at a particular location.

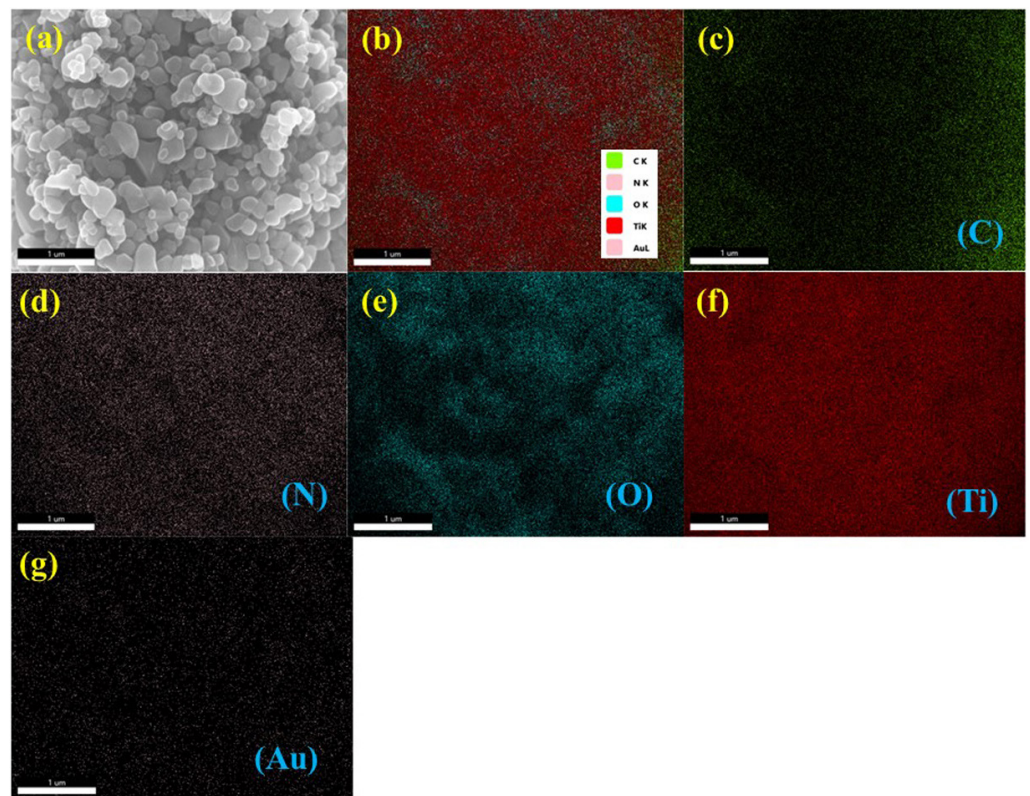


**Fig. 6.** Element mapping of TiO<sub>2</sub> nanoparticles (a), all present elements (b), Carbon (c), Nitrogen (d), Oxygen (e), Titanium (f), and Gold (g)

Element mapping results provide insights into the spatial distribution of carbon, oxygen, titanium, chromium, iron, nickel, and gold elements within the TiO<sub>2</sub> nanoparticles. Coating on the SS 316L substrate. Detailed maps illustrating the composition and concentration of specific elements in different regions of the sample are shown in Figure 6. The element mapping of TiO<sub>2</sub> nanoparticles (a), all elements present in sample (b), Carbon (c), Nitrogen (d), Oxygen (e), Titanium (f), and Gold (g) [16].

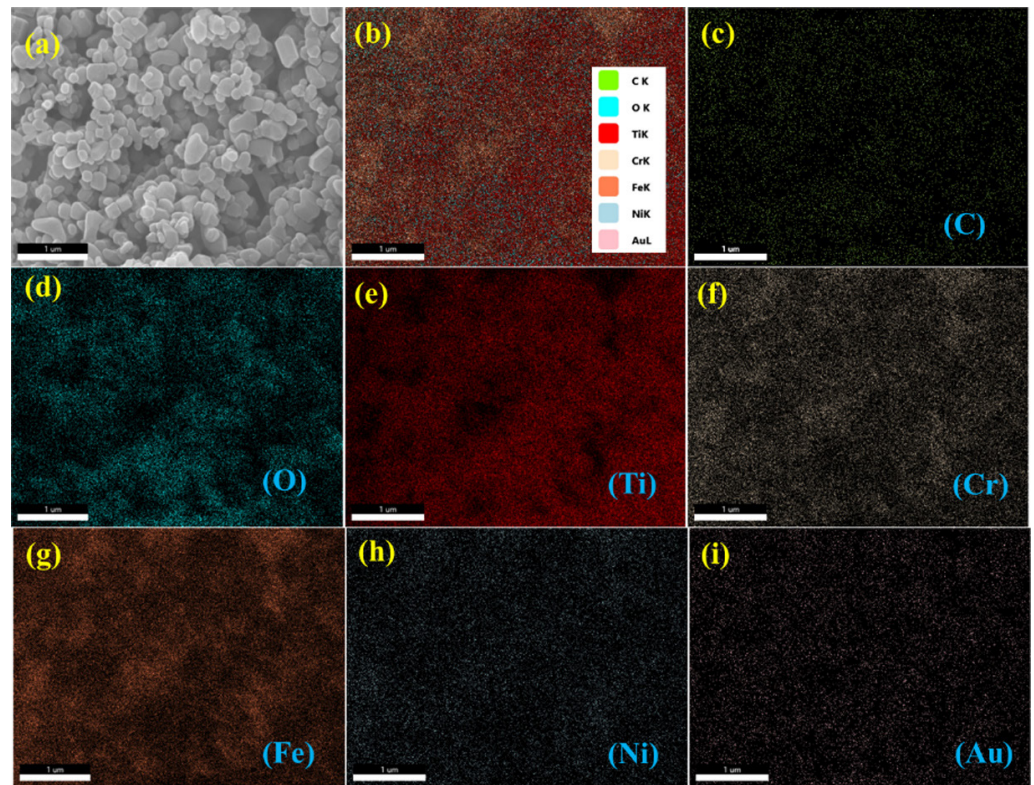


Fig. 7. Element mapping of  $\text{TiO}_2$  nanoparticles coated stainless steel 316L (a), all present elements (b), Carbon (c), Oxygen (d), Titanium (e), Chromium (f), Iron (g), Nickel (h), and Gold (i)

### 3.6 Viability studies

The MTT test was performed to evaluate the in vitro cytotoxicity of  $\text{TiO}_2$  nanoparticles, their coating on SS 316L substrates, and uncoated SS 316L substrates against NIH-3T3 mouse embryonic fibroblast cells. The cell viability graph (see Figure 8) illustrates the relative viability of cells compared to the control (untreated cells) sample for  $\text{TiO}_2$  nanoparticles, uncoated SS 316L substrate, and  $\text{TiO}_2$  nanoparticles coated SS 316L substrate.

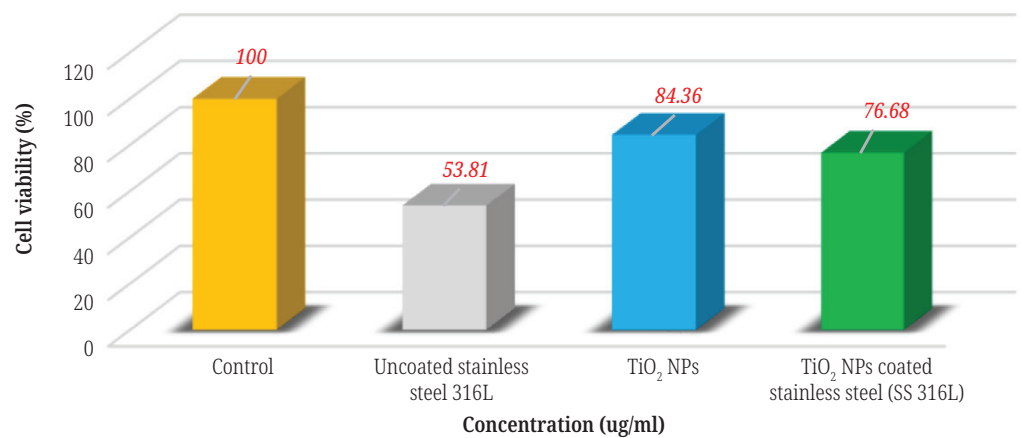
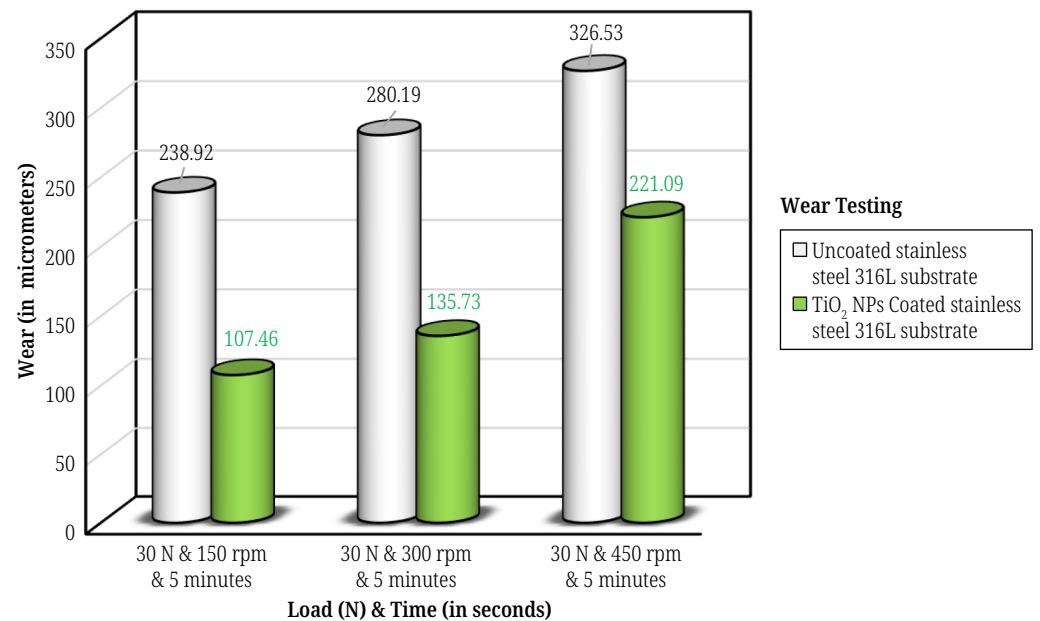


Fig. 8. Cell viability of control, stainless steel 316L uncoated substrate,  $\text{TiO}_2$  nanoparticles, and  $\text{TiO}_2$  nanoparticles coated stainless steel 316L substrate

The viability of fibroblasts serves as an indicator of the toxicity level of the substrate-cell interaction, with higher viability suggesting a less toxic interaction. Cell survival is dependent on attachment, influenced by substrate surface properties such as texture, charge, and rigidity. TiO<sub>2</sub> nanoparticles have been widely recognized for their excellent biocompatibility, meaning they are well-tolerated by living organisms without eliciting adverse reactions. When applied as a coating to the stainless-steel substrate, TiO<sub>2</sub> nanoparticles create a surface that is more conducive to cell adhesion and proliferation. The texture of TiO<sub>2</sub> nanoparticles coated on SS316L substrate provides anchor points for cell attachment, while surface charge facilitates adhesion by promoting interactions with cell membrane receptors. Furthermore, the increased rigidity of TiO<sub>2</sub> nanoparticles coated on the SS 316L substrate influences cellular behaviour, with substrates of optimal stiffness supporting cell spreading and proliferation. These characteristics contribute to enhanced cell attachment and improved viability across various biomedical applications. The results revealed that the relative viability of uncoated SS 316L substrate was 53.81%, whereas for substrate coated with TiO<sub>2</sub> nanoparticles, it was 76.68%, and for TiO<sub>2</sub> nanoparticles alone, it was 84.36%. Remarkably, there was a significant increase of 22.87% in the relative viability of TiO<sub>2</sub> nanoparticle-coated SS 316L substrate compared to the uncoated SS 316L substrate. These findings indicate that TiO<sub>2</sub> nanoparticle coating exhibits superior cell viability compared to the uncoated SS 316L substrate. The enhanced cell viability observed on TiO<sub>2</sub> nanoparticle-coated SS 316L substrates indicated the absence of toxic degradation products and minimized the adverse effects on cellular health and viability, allowing for better cell survival and proliferation, highlighting their potential as coating materials for orthopaedic applications [13], [14], [15].

### 3.7 Wear testing

Wear testing involves analysing the durability and resistance of materials subjected to frictional forces and mechanical stress. The wear rate of the uncoated and TiO<sub>2</sub> nanoparticle-coated stainless steel substrates was evaluated using a ball-on-disc tribometer test.



**Fig. 9.** Wear of uncoated substrate, and TiO<sub>2</sub> nanoparticles coated stainless steel 316L substrate at 150 rpm, 300 rpm, and 450 rpm under 30 N load condition for 5 minutes



The wear rate, expressed as the total height loss per unit sliding time, serves as a key metric for assessing the performance of materials under sliding conditions. The obtained wear rates provided valuable insights into the wear behaviour of the nanoparticle-coated and uncoated stainless-steel substrates. A lower wear rate indicated reduced material loss and improved wear resistance. The wear (in micrometres) of uncoated SS 316L substrate, and  $\text{TiO}_2$  nanoparticle-coated stainless steel 316L substrate at 150 rpm, 300 rpm and 450 rpm under 30 N load conditions for five minutes is shown in Figure 9. The values of maximum wear for uncoated SS 316L substrate were found to be 283.92  $\mu\text{m}$ , 280.19  $\mu\text{m}$ , and 326.53  $\mu\text{m}$ , while for  $\text{TiO}_2$  nanoparticle-coated SS 316L substrate, the maximum wear values were 107.46  $\mu\text{m}$ , 135.73  $\mu\text{m}$ , and 221.09  $\mu\text{m}$  at rotating speeds of 150 rpm, 300 rpm and 450 rpm, respectively. The lowest value of maximum wear obtained is 107.46  $\mu\text{m}$  for coated substrate under 30N load conditions at 150 rpm. The results clearly indicate that the maximum wear of the  $\text{TiO}_2$  nanoparticle-coated substrate is lower compared to the uncoated substrate under various speed and load conditions within the same time period. This suggests that the coating significantly reduces the wear rate, minimizing material loss and surface damage, and enhancing overall durability for orthopaedic applications. [15], [16]. The coefficient of friction (COF), which quantifies the amount of resistance to motion, provides information about the tribological properties of materials, including their resistance to wear and their ability to withstand frictional forces.

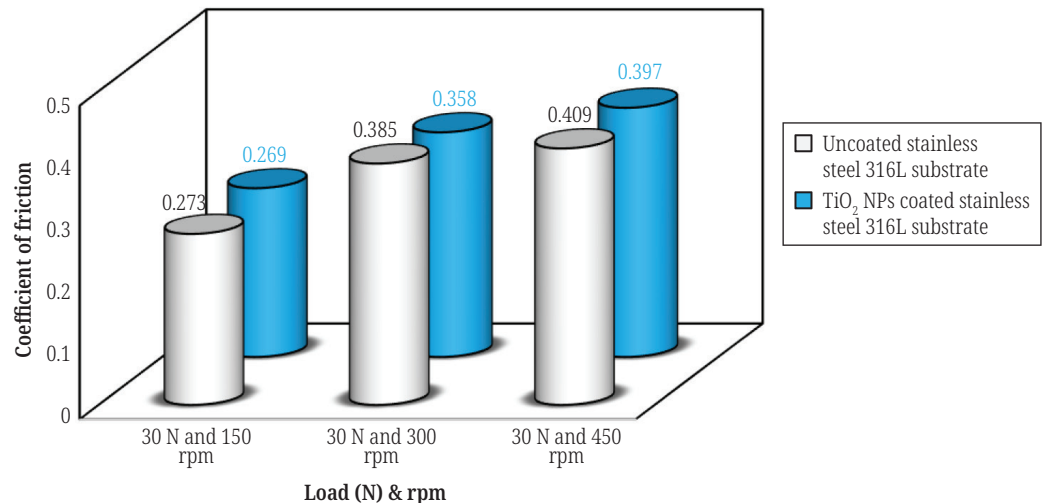


**Fig. 10.** Coefficient of friction (COF) of uncoated substrate, and  $\text{TiO}_2$  nanoparticle-coated stainless steel 316L substrate at 150 rpm, 300 rpm, and 450 rpm under 30 N load condition for five minutes

The COF was measured as the ratio of the frictional force to the normal force acting between the surfaces. A low coefficient of friction is highly favoured as it reduces the chances of micromotion, implant displacement and eventual implant failure. By diminishing frictional forces, the implant becomes more resistant to movement or loosening within the bone or surrounding tissue, thereby guaranteeing prolonged stability and durability. Figure 10 illustrates the values of COF for uncoated and  $\text{TiO}_2$  nanoparticle-coated SS 316L substrate measured at 150 rpm, 300 rpm, and 450 rpm under 30 N load conditions for five minutes. The COF of uncoated SS 316L substrate was found to be 0.273, 0.385 and 0.409, whereas the COF of  $\text{TiO}_2$  nanoparticle-coated SS 316L was 0.269, 0.358 and 0.397. Lower COF values of  $\text{TiO}_2$  nanoparticles coated on SS 316L substrate at 150 rpm under 30 N load conditions indicate reduced friction compared to other samples. The improved mechanical properties exhibited by the  $\text{TiO}_2$  nanoparticle-coated substrate in comparison to its uncoated counterpart

stem from several significant factors. Firstly, the incorporation of TiO<sub>2</sub> nanoparticles enhances surface integrity by augmenting hardness, thereby effectively mitigating deformation and wear. This augmented hardness contributes to the formation of a protective layer, thereby bolstering durability. Additionally, the presence of TiO<sub>2</sub> nanoparticles mitigates friction between sliding surfaces, consequently reducing abrasive wear. Also, TiO<sub>2</sub> nanoparticles also demonstrate better lubricating characteristics, further ameliorating wear and surface damage [16], [17], [18]. A comparison between present work and previously reported work is provided in Table 1.

**Table 1.** Comparison table between figures of merits

	Material Used	Antimicrobial Activity (Z.O.I) <i>E. Coli</i> & <i>S. Aureus</i>	Cytotoxicity (MTT Test)	Wear (Speed & Load)	Corrosion (Current & Potential)
<b>Present work</b>	TiO <sub>2</sub> nanoparticle coating on SS316L	–	MTT assay of cell viability control SS 316L: 53.81% and TiO <sub>2</sub> Coated NCS SS 316L: 76.68%	The values of maximum wear for uncoated SS 316L substrate were found to be 283.92 μm, 280.19 μm, and 326.53 μm while for TiO <sub>2</sub> nanoparticles coated SS 316L substrate the maximum wear values were 107.46 μm, 135.73 μm, and 221.09 μm at rotating speeds of 150 rpm, 300 rpm and, 450 rpm respectively.	–
<b>Ref. [19]</b>	Ag-MgO NCS surface coating on SS 316L	<i>E. coli</i> (+ve control-28 mm, Ag-MgO NCS 37 mm & coated SS 316L Ag-MgO NCS 34 mm, +ve control-26 mm), and <i>S. aureus</i> (+ve control-23 mm, Ag-MgO NCS 32 mm & coated SS 316L Ag-MgO NCS 33 mm, +ve control-21 mm)	MTT assay of cell viability control SS 316L: 55.15% and Ag-MgO Coated NCS SS 316L: 84.26%	Control SS 316L [(Speed-200,350 & 500 rpm), (Wear-257.36, 299.53, & 343.84), (Load-30N)], and Coated Ag-MgO NCS SS 316L [(Speed-200,350 & 500 rpm), (Wear-120.08, 152.38, & 240.36), (Load-30N)].	Control SS 316L ( $I_{corr}$ : 0.03356 uA, $E_{corr}$ : -0.13150 V), and Coated Ag NPs SS 316L ( $I_{corr}$ : 0.02479 uA, $E_{corr}$ : -0.03933), Coated MgO NPs SS 316L ( $I_{corr}$ : 0.12640 uA, $E_{corr}$ : 0.00970), Coated Ag-MgO NCS SS 316L ( $I_{corr}$ : 0.02433 uA, $E_{corr}$ : -0.11999)
<b>Ref. [20]</b>	Silver nanoparticle coating on SS	Over the time period of 24 hours, an Ag-coated SS sample showed a 13-fold reduction in bacteria ( <i>P. aeruginosa</i> ) compared to uncoated SS.	3 day sample mean = 0.0199; 3 day control mean = 0.01867; 7 day sample mean = 0.0222; 7 day control mean = 0.0233.	–	–
<b>Ref. [21]</b>	Ag nanocomposite coatings on 316L SS, a-C and a-C	–	–	19.60 m <sup>3</sup> /cycles for a-C1 wear rate and Ag NCS coatings for a-C: C2 (Ag content 2.97), -12.62 m <sup>3</sup> /cycles, and C3 (Ag content 4.46) 0.002 m <sup>3</sup> per cycle, C4 (Ag content 5.47) 6.12 m <sup>3</sup> per cycle, C5 (Ag content 8.37) 16.92 m <sup>3</sup> per cycle.	Uncoated 316L SS $E_{corr}$ : -340 mV, $I_{corr}$ : 10.30 μA/cm <sup>2</sup> , C1 $E_{corr}$ : -275 mV, $I_{corr}$ : 2.64 μA/cm <sup>2</sup> , C2 $E_{corr}$ : -234 mV, $I_{corr}$ : 0.94 μA/cm <sup>2</sup> , C3 $E_{corr}$ : -160 mV, $I_{corr}$ : 0.63 μA/cm <sup>2</sup> , C4 $E_{corr}$ : -147 mV, $I_{corr}$ : 0.04 μA/cm <sup>2</sup> , C5 $E_{corr}$ : -193 mV, $I_{corr}$ : 0.48 μA/cm <sup>2</sup>

(Continued)

**Table 1.** Comparison table between figures of merits (Continued)

	Material Used	Antimicrobial Activity (Z.O.I) <i>E. Coli</i> & <i>S. Aureus</i>	Cytotoxicity (MTT Test)	Wear (Speed & Load)	Corrosion (Current & Potential)
Ref. [22]	Graphene/zinc oxide nanocomposite	–	Cell viability of GZNC = 80%	–	–
Ref. [23]	Ni-SiC NCs coated on SS 316L	–	–	When compared to an uncoated SS 316L substrate, the wear rate is reduced by 34% with Ni-SiC NCs coating.	When compared to an uncoated SS 316L substrate, the wear rate is reduced by 34% with Ni-SiC NCs coating.
Ref. [24]	Ag nanorods incorporated CaSiO <sub>3</sub> powder	Zone of inhibition (ZOI): <i>E. coli</i> bacteria Ag-CaSiO <sub>3</sub> = 1.5 cm, Ag nanorods = 2.6 cm, and <i>S. aureus</i> Ag-CaSiO <sub>3</sub> = 1.2 cm, Ag nanorods = 2.8 cm	–	–	–

On the basis of comparison table, it is quite clear that the present study has major potential in terms of orthopaedic implant.

#### 4 CONCLUSION

In this study, TiO<sub>2</sub> nanoparticles were coated on SS 316L substrates through the spin coating technique and evaluated for their potential to be used as orthopaedic implant coatings. Various characterization techniques, such as X-ray diffraction, Fourier transform infrared spectroscopy, and scanning electron microscopy with energy dispersive X-ray analysis, were used to confirm the composition, crystallinity, and morphology of the synthesised TiO<sub>2</sub> nanoparticles and their coating on the SS 316L substrate. The SEM and XRD results confirmed the synthesised TiO<sub>2</sub> nanoparticles have a spherical shape and an average size of approximately 23 nanometres. SEM images verified the uniformity and morphology of the TiO<sub>2</sub> nanoparticle-coatings on the surface of the SS 316L substrate. Cell viability studies of TiO<sub>2</sub> nanoparticle-coated SS 316L substrate against embryonic fibroblast cell lines were carried out using the MTT assay and compared to the control, TiO<sub>2</sub> nanoparticles, uncoated with SS 316L substrate. The results indicate a significant improvement (22.87%) in the cell viability of the TiO<sub>2</sub> nanoparticle-coated substrate compared to the uncoated SS 316L substrate. Furthermore, the wear and friction resistance of the uncoated and TiO<sub>2</sub> nanoparticle-coated SS 316L substrate were assessed using the ball-on-disc tribometer method at various speeds, viz., 150 rpm, 300 rpm and 450 rpm, under 30N load conditions for five minutes. A lower wear rate and friction resistance with respect to uncoated SS 316L substrates were measured for all the speeds, which testify to better wear protection of the TiO<sub>2</sub> nanoparticle-coated SS 316L substrates compared to the uncoated one. The findings suggest that the coated substrates hold promise for enhancing the suitability of TiO<sub>2</sub> nanoparticle coating on implants for orthopaedic applications, addressing critical concerns such as biocompatibility, cell viability, tissue integration and implant longevity. Further research is needed to investigate the long-term implications and in vivo performance of the TiO<sub>2</sub> nanoparticle-coating on the SS 316L orthopaedic implant for clinical use.



## 5 ACKNOWLEDGEMENT

First and foremost, we extend sincere gratitude to our supervisor whose guidance and invaluable expertise have played a pivotal role in shaping the direction and enhancing the quality of this study. We thank the Department of Bio- and Nano Technology, Central Instrumental Lab (CIL), Guru Jambheshwar University of Science and Technology, Hisar for providing the necessary resources and facilities that supported the various phases of our research journey.

## 6 REFERENCES

- [1] J. Quinn, R. McFadden, C.-W. Chan, and L. Carson, "Titanium for orthopedic applications: An overview of surface modification to improve biocompatibility and prevent bacterial biofilm formation," *iScience*, vol. 23, no. 11, p. 101745, 2020. <https://doi.org/10.1016/j.isci.2020.101745>
- [2] M. S. Jadon, G. Bhanjana, N. Dilbaghi, N. K. Singhal, and S. Kumar, "Fabrication and evaluation of silver-doped magnesium oxide nanocomposite coatings for orthopaedics applications," *J Alloys Compd*, vol. 972, p. 172848, 2024. <https://doi.org/10.1016/j.jallcom.2023.172848>
- [3] O. U. Akakuru, Z. M. Iqbal, and A. Wu, "TiO<sub>2</sub> nanoparticles: Properties and applications," *Wiley*, pp. 1–66, 2020. <https://doi.org/10.1002/9783527825431.ch1>
- [4] S. Noreen, E. Wang, H. Feng, and Z. Li, "Functionalization of TiO<sub>2</sub> for better performance as orthopedic implants," *Materials*, vol. 15, no. 19, p. 6868, 2022. <https://doi.org/10.3390/ma15196868>
- [5] M. Kheirkhah, M. Fathi, H. R. Salimijazi, and M. Razavi, "Surface modification of stainless steel implants using nanostructured forsterite (Mg<sub>2</sub>SiO<sub>4</sub>) coating for biomaterial applications," *Surf Coat Technol*, vol. 276, pp. 580–586, 2015. <https://doi.org/10.1016/j.surfcoat.2015.06.012>
- [6] Z. Hayati, B. Hoomehr, F. Khalesi, and K. Raeissi, "Synthesis and electrophoretic deposition of TiO<sub>2</sub>-SiO<sub>2</sub> composite nanoparticles on stainless steel substrate," *J Alloys Compd*, vol. 931, p. 167619, 2023. <https://doi.org/10.1016/j.jallcom.2022.167619>
- [7] Z. Kielan-Grabowska *et al.*, "Improvement of properties of stainless steel orthodontic archwire using TiO<sub>2</sub>:Ag coating," *Symmetry (Basel)*, vol. 13, no. 9, p. 1734, 2021. <https://doi.org/10.3390/sym13091734>
- [8] V. Suresh and A. Jegan, "Experimental studies on wear and corrosion resistance of pulse electrodeposited Ni-TiO<sub>2</sub> nanocomposite coatings on AISI 304 stainless steel," *Mater Res Express*, vol. 9, no. 12, p. 126401, 2022. <https://doi.org/10.1088/2053-1591/acabb2>
- [9] A. Nabhan, M. Taha, and N. M. Ghazaly, "Filler loading effect of Al<sub>2</sub>O<sub>3</sub>/TiO<sub>2</sub> nanoparticles on physical and mechanical characteristics of dental base composite (PMMA)," *Polym Test*, vol. 117, p. 107848, 2023. <https://doi.org/10.1016/j.polymertesting.2022.107848>
- [10] K. Santhi, M. Navaneethan, S. Harish, S. Ponnusamy, and C. Muthamizhchelvan, "Synthesis and characterization of TiO<sub>2</sub> nanorods by hydrothermal method with different pH conditions and their photocatalytic activity," *Appl. Surf. Sci.*, vol. 500, p. 144058, 2020. <https://doi.org/10.1016/j.apsusc.2019.144058>
- [11] H. Varol Özkavak and H. Asil Uğurlu, "Coating TiO<sub>2</sub> film using the spin method of AISI 304 stainless steel and investigation of the structural properties," *International Journal of Innovative Engineering Applications*, vol. 6, no. 1, pp. 97–102, 2022. <https://doi.org/10.46460/ijiea.1070575>

- [12] F. Temerov, L. Ammosova, J. Haapanen, J. M. Mäkelä, M. Suvanto, and J. J. Saarinen, "Protective stainless steel micropillars for enhanced photocatalytic activity of TiO<sub>2</sub> nanoparticles during wear," *Surf. Coat. Technol.*, vol. 381, p. 125201, 2020. <https://doi.org/10.1016/j.surfcoat.2019.125201>
- [13] J. M. Abisharani, R. DineshKumar, S. Devikala, M. Arthanareeswari, and S. Ganesan, "Influence of 2,4-Diamino-6-Phenyl-1-3-5-triazine on bio synthesized TiO<sub>2</sub> dye-sensitized solar cell fabricated using poly (ethylene glycol) polymer electrolyte," *Mater Res. Express*, vol. 7, no. 2, p. 025507, 2020. <https://doi.org/10.1088/2053-1591/ab7066>
- [14] C. C. Wachesk, S. H. Seabra, T. A. T. Dos Santos, V. J. Trava-Airoldi, A. O. Lobo, and F. R. Marciano, "In vivo biocompatibility of diamond-like carbon films containing TiO<sub>2</sub> nanoparticles for biomedical applications," *J. Mater. Sci. Mater. Med.*, vol. 32, no. 9, p. 117, 2021. <https://doi.org/10.1007/s10856-021-06596-6>
- [15] S. Durdu *et al.*, "Characterization and investigation of properties of copper nanoparticle coated TiO<sub>2</sub> nanotube surfaces on Ti6Al4V alloy," *Mater. Chem. Phys.*, vol. 292, p. 126741, 2022. <https://doi.org/10.1016/j.matchemphys.2022.126741>
- [16] D. J. Aldabagh, T. L. Alzubadi, and A. F. Alhuwaizi, "Tribology of coated 316L SS by various nanoparticles," *Int. J. Biomater.*, vol. 2023, pp. 1–13, 2023. <https://doi.org/10.1155/2023/6676473>
- [17] A. Gnanavelbabu, E. Vinothkumar, N. S. Ross, and M. Prahadeeswaran, "Investigating the wear performance of AZ91D magnesium composites with ZnO, MnO, and TiO<sub>2</sub> nanoparticles," *The International Journal of Advanced Manufacturing Technology*, vol. 129, nos. 9–10, pp. 4217–4237, 2023. <https://doi.org/10.1007/s00170-023-12502-x>
- [18] R. Gecu, B. Birol, and M. Özcan, "Improving wear and corrosion protection of AISI 304 stainless steel by Al<sub>2</sub>O<sub>3</sub>-TiO<sub>2</sub> hybrid coating via sol-gel process," *Transactions of the IMF*, vol. 100, no. 6, pp. 324–332, 2022. <https://doi.org/10.1080/00202967.2022.2117884>
- [19] M. S. Jadon, G. Bhanjana, N. Dilbaghi, N. K. Singhal, and S. Kumar, "Fabrication and evaluation of silver-doped magnesium oxide nanocomposite coatings for orthopaedics applications," *Journal of Alloys and Compounds*, vol. 972, p. 172848, 2024. <https://doi.org/10.1016/j.jallcom.2023.172848>
- [20] P. DeVasConCellos, S. Bose, H. Beyenal, A. Bandyopadhyay, and L. G. Zirkle, "Antimicrobial particulate silver coatings on stainless steel implants for fracture management," *Materials Science and Engineering: C*, vol. 32, no. 5, pp. 1112–1120, 2012. <https://doi.org/10.1016/j.msec.2012.02.020>
- [21] V. S. Dhandapani, E. Thangavel, M. Arumugam, K. S. Shin, V. Veeraraghavan, S. Y. Yau, and D. E. Kim, "Effect of Ag content on the microstructure, tribological and corrosion properties of amorphous carbon coatings on 316L SS," *Surface and Coatings Technology*, vol. 240, pp. 128–136, 2014. <https://doi.org/10.1016/j.surfcoat.2013.12.025>
- [22] S. Kulshrestha, S. Khan, R. Meena, B. R. Singh, and A. U. Khan, "A graphene/zinc oxide nanocomposite film protects dental implant surfaces against cariogenic Streptococcus mutans," *Biofouling*, vol. 30, no. 10, p. 12811294, 2014. <https://doi.org/10.1080/08927014.2014.983093>
- [23] N. M. Dawood, N. S. Radhi, and Z. S. Al-Khafaji, "Investigation corrosion and wear behavior of Nickel-Nano silicon carbide on stainless steel 316L," *Materials Science Forum*, vol. 1002, pp. 33–43, 2020. <https://doi.org/10.4028/www.scientific.net/MSF.1002.33>
- [24] C. Moseke, U. Gbureck, P. Elter, P. Drechsler, A. Zoll, R. Thull, and A. Ewald, "Hard implant coatings with antimicrobial properties," *Journal of Materials Science: Materials in Medicine*, vol. 22, no. 12, pp. 2711–2720, 2011. <https://doi.org/10.1007/s10856-011-4457-6>

## 7 AUTHORS

**Mr. Manjit Singh Jadon** did his bachelor degree in biomedical engineering from Guru Jambheshwar University of Science and Technology Hisar, India. Thereafter he joined as M.Tech student at IIT Madras. After completing his masters from IIT Madras, he joined as Ph.D. Scholar in Nano Science and Technology at Guru Jambheshwar University of Science and Technology, Hisar, India. Presently he is pursuing his Ph.D. on fabrication and evaluation of nanomaterial coated novel implant materials (E-mail: [msjadon1910@gjust.org](mailto:msjadon1910@gjust.org)).

**Dr. Sandeep Kumar** is presently working as Professor, Department of Physics, Punjab Engineering College (Deemed to be University), Chandigarh and was earlier faculty at the Department of Bio and Nano Technology, Guru Jambheshwar University of Science and Technology, Hisar, Haryana, India. Dr. Kumar did his PhD from Panjab University, Chandigarh. His research interests include synthesis of nanomaterials, nanocarriers for healthcare applications, nanomaterials-based sensors, biomaterials, and nanotoxicology. Professor Kumar has guided 10 PhD students, 2 Post Docs and more than 40 M Tech/PG students. He has one patent and more than 170 research papers in many reputed international journals with high impact factors (Phone: 99623-42017).